Improving the accuracy performance of phase-shifting profilometry for the measurement of objects in motion

Lei Lu, Jiangtao Xi,* Yanguang Yu, and Qinghua Guo

School of Electrical Computer and Telecommunications Engineering, University of Wollongong, Wollongong, NSW 2522, Australia
**Corresponding author: jiangtao@uow.edu.au*

Received July 29, 2014; revised October 5, 2014; accepted October 10, 2014;
posted October 14, 2014 (Doc. ID 220038); published November 26, 2014

This Letter presents a new approach to reducing the errors associated with the shape measurement of a rigid object in motion by means of phase-shifting profilometry. While the work previously reported is only valid for the case of two-dimensional (2-D) movement, the proposed method is effective for a situation in which the object moves in a three-dimensional (3-D) space. First, a new model is proposed to describe the fringe patterns reflected from the object, which is subject to 3-D movement. Then, an iterative least-squares algorithm is presented to estimate the phase map. Experiments show that, in contrast to conventional phase-shifting profilometry, the proposed method is capable of significantly reducing the error caused by the 3-D movement of the object.

OCIS codes: (120.6650) Surface measurements, figure; (120.5050) Phase measurement; (100.2650) Fringe analysis.
http://dx.doi.org/10.1364/OL.39.006715

Phase-shifting profilometry (PSP) is one of the most promising approaches for non-destructive 3-D shape measurement. However, while multiple fringe patterns are projected, the object must be kept static. Measurement errors will occur if the object moves.

The above problem can be addressed from a number of aspects. Zhang and Yau proposed a modified two-plus-one phase-shifting algorithm to address the problem by projecting two sinusoidal fringe patterns and a uniform flat image [1]. As the height information is only contained in the two sinusoidal fringe patterns, the error due to motion is smaller than with traditional PSP. However, the error still occurs when the object moves during the projections of the two sinusoidal fringe patterns. Wang *et al.*, proposed the use of a high-speed camera recording 5000 frames per second to measure the moving object [2]. The object can be considered as static during the projection of the phase-shifted fringe patterns. However, use of such high-speed equipment implies a significant increase in the cost of implementing the system. Based on an analysis of the influence on the fringe patterns caused by the movement, Lu *et al.* proposed a method to reduce the error caused by the rigid object's movement [3]. However, the method presented in [3] is only applicable in the case of 2-D movement of the object, which is limited in terms of practical applications.

In this Letter, a new method is proposed to cope with the errors caused by the 3-D movement of the object in PSP. In particular, we consider the case that the object has a rigid shape, and that the movement consists of a translation in the direction of height and a 2-D movement in the plane perpendicular to the direction of height. The details are described below.

When the object is kept static and N-step PSP is used, the fringe patterns acquired from the reference plane and the object can be expressed as

$$\begin{cases} s_n(x,y) = a + b\cos[\omega(x,y) + 2\pi n/N] \\ d_n(x,y) = a + b\cos[\omega(x,y) + \Phi(x,y) + 2\pi n/N], \end{cases} \quad (1)$$

where $n = 1, 2, \ldots, N$; $s_n(x,y)$ and $d_n(x,y)$ are the n-th fringe patterns on the reference plane and the object, respectively, a is the background intensity resulting from pattern offset and ambient light, and b is the amplitude of the intensity of the sinusoidal fringe patterns. As we are only considering the constant background intensity and objects with diffuse surfaces, a and b can be seen as constant, $\omega(x,y)$ is the phase value on the reference plane, and $\Phi(x,y)$ is the phase difference between the object and the reference plane. When $\Phi(x,y)$ is obtained, the shape of the object can be calculated by:

$$h(x,y) = \frac{l_0\Phi(x,y)}{\Phi(x,y) - 2\pi f_0 d_0}, \quad (2)$$

where $h(x,y)$ is the height distribution of object, l_0 is the distance between the camera and the reference plane, f_0 is the spatial frequency of the fringe patterns, and d_0 is the distance between the camera and the projector.

Now let us consider the case where the object is subject to a 3-D movement and the height distribution changes from $h(x,y)$ to $\tilde{h}(x,y)$. Due to the rigid nature of the subject's shape, a point (x,y) on the object is moved to (u,v) following the relationship below:

$$\begin{bmatrix} x \\ y \\ h(x,y) \end{bmatrix} = \mathbf{R}\begin{bmatrix} u \\ v \\ \tilde{h}(u,v) \end{bmatrix} + \mathbf{T},$$
$$\begin{bmatrix} u \\ v \\ \tilde{h}(u,v) \end{bmatrix} = \bar{\mathbf{R}}\begin{bmatrix} x \\ y \\ h(x,y) \end{bmatrix} + \bar{\mathbf{T}}, \quad (3)$$

where $\mathbf{R}$, $\bar{\mathbf{R}}$, $\mathbf{T}$, and $\bar{\mathbf{T}}$ are referred to as rotation matrixes and translation vectors. As we are only considering the case that the movement is the combination of a translation in the direction of height and a 2-D movement in the plane perpendicular to the direction of height, we have:

$$\mathbf{R}=\begin{bmatrix} r_{11} & r_{12} & 0\\ r_{21} & r_{22} & 0\\ 0 & 0 & 1\end{bmatrix},\qquad \mathbf{T}=\begin{bmatrix} t_1\\ t_2\\ t_3\end{bmatrix},$$
$$\bar{\mathbf{R}}=\begin{bmatrix} \bar{r}_{11} & \bar{r}_{12} & 0\\ \bar{r}_{21} & \bar{r}_{22} & 0\\ 0 & 0 & 1\end{bmatrix},\qquad \bar{\mathbf{T}}=\begin{bmatrix} \bar{t}_1\\ \bar{t}_2\\ \bar{t}_3\end{bmatrix}. \tag{4}$$

Because the movement in the direction of height is exclusively a translation, we have:

$$\tilde{h}^{x-y}(u,v)=h^{x-y}(x,y)+\bar{t}_3=h^{x-y}[f(u,v),g(u,v)]+\bar{t}_3, \tag{5}$$

where x–y denotes the coordinate system in which the functions are defined and

$$f(u,v)=r_{11}u+r_{12}v+t_1,\qquad g(u,v)=r_{21}u+r_{22}v+t_2. \tag{6}$$

Without loss of generality, (u,v) can be replaced by (x,y). Therefore, Eq. (5) yields the following:

$$\tilde{h}^{x-y}(x,y)=h^{x-y}[f(x,y),g(x,y)]+\bar{t}_3. \tag{7}$$

We define the object fringe patterns after movement as

$$\tilde{d}_n^{x-y}(x,y)=a+b\cos[\omega(x,y)+\tilde{\Phi}(x,y)+2\pi n/N], \tag{8}$$

where $\tilde{\Phi}(x,y)$ is the phase difference at point (x,y) after movement. Generally, l_0 is much larger than the measured object and the height variation $\bar{t}_3$. The phase variations caused by $\bar{t}_3$ for each point of object are approximately the same. Because of Eq. (7), we have

$$\tilde{\Phi}(x,y)=\Phi[f(x,y),g(x,y)]+\Phi', \tag{9}$$

where Φ' is the phase variation caused by $\bar{t}_3$. By inserting Eq. (9) into Eq. (8), we get

$$\tilde{d}_n^{x-y}(x,y)=a+b\cos\{\omega(x,y)+\Phi[f(x,y),g(x,y)]+\Phi'+2\pi n/N\}. \tag{10}$$

Note that in order to avoid the phase ambiguity Φ' is limited to less than 2π, which requires the object movement to be smaller than a single fringe. Now, let us consider Eq. (10) in the new coordinate system $\xi-\eta$ following the relationship below:

$$\begin{bmatrix} x\\ y\end{bmatrix}=\begin{bmatrix} \bar{r}_{11} & \bar{r}_{12}\\ \bar{r}_{21} & \bar{r}_{22}\end{bmatrix}\begin{bmatrix} \xi\\ \eta\end{bmatrix}+\begin{bmatrix} \bar{t}_1\\ \bar{t}_2\end{bmatrix}. \tag{11}$$

In $\xi-\eta$ coordinate system, Eq. (10) becomes

$$\tilde{d}_n^{\xi-\eta}(\xi,\eta)=\tilde{d}_n^{x-y}[\bar{f}(\xi,\eta),\bar{g}(\xi,\eta)]=a+b\cos\{\omega[\bar{f}(\xi,\eta),\bar{g}(\xi,\eta)]+\Phi(\xi,\eta)+\Phi'+2\pi n/N\}, \tag{12}$$

where

$$\bar{f}(u,v)=\bar{r}_{11}u+\bar{r}_{12}v+\bar{t}_1,\qquad \bar{g}(u,v)=\bar{r}_{21}u+\bar{r}_{22}v+\bar{t}_2. \tag{13}$$

By using (x,y) to replace (ξ,η) and extending Eq. (12) to N-step PSP, we yield the following:

$$\tilde{d}_n(x,y)=\tilde{d}_n^{x-y}[\bar{f}_n(x,y),\bar{g}_n(x,y)]=a+b\cos\{\omega[\bar{f}_n(x,y),\bar{g}_n(x,y)]+\Phi(x,y)+\Phi'_n+2\pi n/N\}. \tag{14}$$

Equation (14) describes the influence of the 3-D movement on the fringe patterns. To simplify the expression, Eq. (14) can be rewritten as follows:

$$\tilde{d}_n(x,y)=a+b\cos[\omega'_n(x,y)+\Phi(x,y)+\delta_n], \tag{15}$$

where $\omega'_n(x,y)=\omega[\bar{f}_n(x,y),\bar{g}_n(x,y)]$. This can be obtained by the fringe patterns of the reference plane and Eq. (13), $\delta_n=\Phi'_n+2\pi n/N$ is the phase shift amount caused by the phase shift of PSP and height variations $\bar{t}_3$ for each step, which is unknown in advance. In order to obtain $\Phi(x,y)$, we must estimate the value of δ_n. Inspired by the methods presented in [4–6], which can extract the random phase shifts for other applications, we propose to employ an iterative least-squares approach to obtain δ_n and $\Phi(x,y)$. The proposed method starts from an initial value of $\delta_n=2\pi n/N$ and can be implemented by taking the following steps.

Step 1: Estimate $\Phi(x,y)$ when an estimation of δ_n is available (it takes the initial value for the first iteration). To this end, we rewrite Eq. (15) as

$$\tilde{d}_n(x,y)=a+B(x,y)\cos\tau+C(x,y)\sin\tau, \tag{16}$$

where $B(x,y)=b\cos\Phi(x,y)$, $C(x,y)=-b\sin\Phi(x,y)$, and $\tau=\omega'_n(x,y)+\delta_n$. Assuming that there are M pixels in one fringe pattern, and when δ_n is known, there are $2M+1$ unknowns and MN equations in Eq. (16). When $N\geq 3$, the unknowns can be obtained by the overdetermined least-squares method. We apply Eq. (14) to the measured fringe patterns $\tilde{d}_n^{x-y}$ to obtain $d_n^m(x,y)$; then, the sum of the squared error in each pixel is

$$S(x,y)=\sum_{n=1}^{N}[\tilde{d}_n(x,y)-d_n^m(x,y)]^2. \tag{17}$$

Based on Eq. (17), the least-squares criteria satisfy that $\partial S(x,y)/\partial a=0$, $\partial S(x,y)/\partial B(x,y)=0$, and $\partial S(x,y)/\partial C(x,y)=0$, and yields the following:

$$\mathbf{X}(x,y)=\mathbf{A}^{-1}(x,y)\mathbf{B}(x,y), \tag{18}$$

where

$$\mathbf{A}(x,y)=\begin{bmatrix} N & \sum_{n=1}^{N}\cos\tau & \sum_{n=1}^{N}\sin\tau \\ \sum_{n=1}^{N}\cos\tau & \sum_{n=1}^{N}\cos & \frac{1}{2}\sum_{n=1}^{N}\sin 2\tau \\ \sum_{n=1}^{N}\sin\tau & \frac{1}{2}\sum_{n=1}^{N}\sin 2\tau & \sum_{n=1}^{N}\sin^2\tau \end{bmatrix}, \tag{19}$$

$$\mathbf{X}(x,y)=[\,a \quad B(x,y) \quad C(x,y)\,]^T, \tag{20}$$

$$\mathbf{B}(x,y)=\begin{bmatrix} \sum_{n=1}^{N}d_n^m(x,y) & \sum_{n=1}^{N}\cos\tau\times d_n^m(x,y) & \sum_{n=1}^{N}\sin\tau\times d_n^m(x,y) \end{bmatrix}^T. \tag{21}$$

From Eqs. (18)–(21), the unknowns a, $B(x,y)$, and $C(x,y)$ can be solved and $\Phi(x,y)$ can be determined:

$$\Phi(x,y)=\tan^{-1}[-C(x,y)/B(x,y)]. \tag{22}$$

Step 2: Estimate δ_n by the least-squares method using $\Phi(x,y)$ estimated in Step 1. For this purpose, Eq. (15) can also be rewritten as

$$\tilde{d}_n(x,y)=a+B'_n\cos\tau'+C'_n\sin\tau', \tag{23}$$

where $B'_n=b\cos\delta_n$, $C'_n=-b\sin\delta_n$, and $\tau'=\omega'_n(x,y)+\Phi(x,y)$. The sum of the squares error in each frame is:

$$S'_n=\sum_{(x,y)}[\tilde{d}_n(x,y)-d_n^m(x,y)]^2. \tag{24}$$

The least-squares solution, which minimizes S'_n, is:

$$\mathbf{X}'_n=\mathbf{A}'^{-1}_n\mathbf{B}'_n, \tag{25}$$

where

$$\mathbf{A}'_n=\begin{bmatrix} M & \sum_{x,y}\cos\tau' & \sum_{x,y}\sin\tau' \\ \sum_{x,y}\cos\tau' & \sum_{x,y}\cos^2\tau' & \frac{1}{2}\sum_{x,y}\sin 2\tau' \\ \sum_{x,y}\sin\tau' & \frac{1}{2}\sum_{x,y}\sin 2\tau' & \sum_{x,y}\sin^2\tau' \end{bmatrix}, \tag{26}$$

$$\mathbf{X}'_n=[\,a \quad B'_n \quad C'_n\,]^T, \tag{27}$$

$$\mathbf{B}'_n=\begin{bmatrix} \sum_{x,y}d_n^m(x,y) & \sum_{x,y}\cos\tau'\times d_n^m(x,y) & \sum_{x,y}\sin\tau'\times d_n^m(x,y) \end{bmatrix}^T. \tag{28}$$

Thus, the unknowns a, B'_n, and C'_n can be obtained by Eqs. (25)–(28). Then, δ_n can be calculated by:

$$\delta_n=\tan^{-1}[-C'_n/B'_n]. \tag{29}$$

The two steps described above are repeated in the way that δ_n estimated from Step 2 is employed in Step 1 to obtain a better estimation of $\Phi(x,y)$, and $\Phi(x,y)$ obtained in Step 1 is utilized in Step 2 to yield a better estimation of δ_n. The iterative process will stop when the convergence condition is met:

$$|(\delta_n^k-\delta_1^k)-(\delta_n^{k-1}-\delta_1^{k-1})|<\varepsilon. \tag{30}$$

Then, $\Phi(x,y)$ will be taken as the correct phase distribution. In the above, k is the number of iterations and ε is the accuracy requirement, e.g., 10^{-4}. In the experiments presented below, we found that a very good convergence can always be achieved, e.g., k is around 10 when $\varepsilon=10^{-4}$.

Experiments have been carried out to verify the proposed method, where the object is the mask shown in Fig. 1(a) and the PSP is the traditional 3-step method. The object was moved on a step-by-step basis in order to emulate the instantaneous positions of the object when the multiple image patterns are recorded. In practice, the shutter of the camera must be fast enough to avoid blurriness in the captured images. As the camera in our laboratory is not fast enough, we kept the object static at each step when the fringe patterns were recorded.

In order to obtain $\Phi(x,y)$ from Eq. (15), $\omega'_n(x,y)$ should be available. To this end, we should obtain $(\bar{r}_{11},\bar{r}_{12},\bar{r}_{21},\bar{r}_{22},\bar{t}_1,\bar{t}_2)$ in Eq. (13). Three marks are employed and placed on the object, as shown in Fig. 1(a). The centers of the marks are extracted using the same approach described in [3], which are used as the corresponding points between multiple fringe patterns. As Eqs. (3) and (4) show that $\bar{t}_3$ is independent of $(\bar{r}_{11},\bar{r}_{12},\bar{r}_{21},\bar{r}_{22},\bar{t}_1,\bar{t}_2)$, the method described in [3] can be employed to obtain $(\bar{r}_{11},\bar{r}_{12},\bar{r}_{21},\bar{r}_{22},\bar{t}_1,\bar{t}_2)$. The following experiments have been conducted:

Experiment 1: We applied the traditional 3-step PSP to the mask when the mask is kept static. The measurement result is shown in Fig. 1(e), which matches our expectations of the traditional 3-step PSP.

Experiment 2: Then, we moved the object in the direction of height for 3 mm and 4 mm in the second and third step of PSP, respectively. The result of traditional PSP is shown in Fig. 1(b); there are obvious errors. When the proposed algorithm is applied to the case where the object is moved by the same amount as above, a significant improvement can be obtained, as shown in Fig. 1(f).

Experiment 3: The object is rotated clockwise in the x–y plane for 0.0599 rad and moved in the direction of height for 5 mm in the second step of PSP; then, the object is rotated clockwise in the x–y plane for 0.0256 rad, and moved in the direction of height for 3 mm in the third step of PSP. The result from the traditional PSP is shown in Fig. 1(c), and shows significant errors. With the proposed algorithm, the result is depicted in Fig. 1(g); it also shows significant improvement.

Experiment 4: The object is moved 3 mm in the x-direction, 5 mm in y-direction, 3 mm in the direction of height, and rotated clockwise in the x–y plane for 0.0295 rad in the second step of PSP. In the third step of PSP, the object is moved 2 mm in the x-direction, 4 mm in y-direction, 2 mm in the direction of height, and rotated clockwise for 0.0277 rad in the x–y plane. Figure 1(d) shows the result from traditional PSP and significant errors occur. The result with the proposed

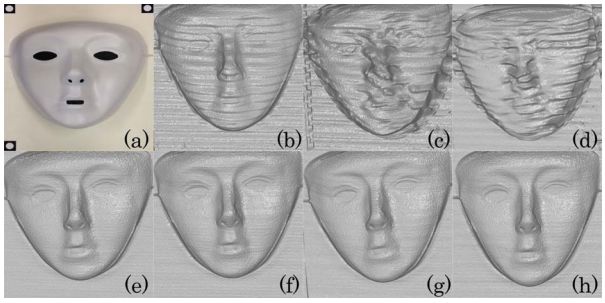

Fig. 1. Comparison of the measurement results of traditional PSP and the proposed method.

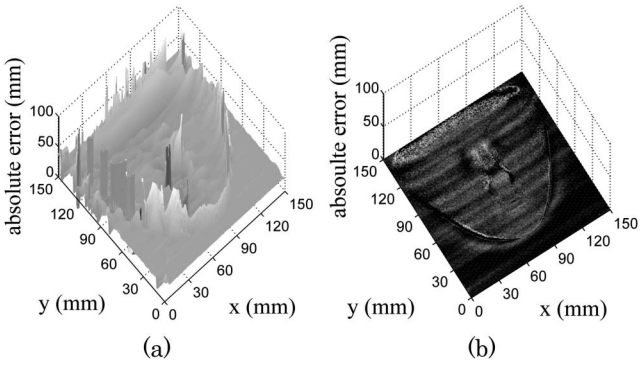

Fig. 2. (a) and (b) The absolute error for Figs. 1(d) and 1(h).

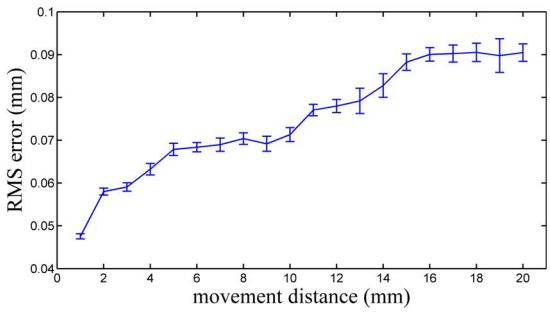

Fig. 3. Relationship between the accuracy of the proposed method and the movement distance in the direction of height.

algorithm is shown in Fig. 1(h), again demonstrating significant improvement.

In order to evaluate the performance of the proposed algorithm, we also computed the root mean square (RMS) errors of the height for all of the points on the object surface, the iterative times, and the height offset for the above experiments. The results are shown in Table 1. As the exact shape of the mask is not available, the reconstructed result for the static object in Fig. 1(e) is used as the reference for our computation. Table 1 shows that the proposed method has significant accuracy improvement and fast convergence.

Figure 2 shows the comparison of the absolute errors for the results shown in Figs. 1(d) and 1(h). It can be seen that the absolute error in Fig. 2(b), using the proposed method, is significantly smaller than the error of the traditional PSP in Fig. 2(a).

We also studied how the amount of movement impacts the RMS error; the result is shown in Fig. 3. In the second and third steps of PSP, the object moves the same distance, and the movement distance in Fig. 3 is the sum of the movement of the two steps. For each movement, 8 experiments are carried out. Figure 3 shows the mean of the RMS errors. The error bars give the standard deviation for the 8 experiments at each movement distance. It is seen that RMS error slightly increases with the movement distance. This may be due to the influence of the geometric structure of the system, as we only used the ideal model for the system structure, the camera, and the projector. It is expected that the error can be reduced by accurately calibrating the system [7,8].

The computational cost associated with the proposed method was also analyzed. The wrapped phase extraction in Eqs. (18)–(22) is most time consuming due to a matrix inversion for each pixel of the fringe patterns. However, parallel computing can be independently implemented for each individual point. We employed such an approach using Matlab on a Dell Vostro 470 computer with 3.4 GHz CPU and 8 G memory, and it took 0.41 seconds to complete one iteration of Step 1 and Step 2 of the proposed algorithm for the fringe pattern of 500 pixels by 500 pixels. It is expected that the time can be further reduced if dedicated hardware is employed [9].

Table 1. Accuracy and Iterative Times ($\varepsilon = 10^{-4}$)

Experiment Number	RMS Errors (Traditional PSP) (mm)	RMS Errors (Proposed Method) (mm)	Iterative Times	Height Offset (mm)
Experiment 2	10.385	0.071	9	0.002
Experiment 3	62.946	0.089	12	0.006
Experiment 4	57.174	0.083	14	0.004

In summary, a new approach has been proposed to determine the phase map of phase-shifted fringe patterns reflected from a rigid object subject to a 3-D movement. First, a new model is presented to describe the fringe patterns influenced by the 3-D movement. Then, an iterative least-squares method is proposed, which is able to estimate the correct phase map without requiring the knowledge of the height variations. The estimated phase map can be used to reconstruct the 3-D shape with improved accuracy performance in comparison to a conventional PSP. Experimental results are also presented to verify the effectiveness of the proposed method.

References

1. S. Zhang and S. T. Yau, Opt. Eng. **46**, 113603 (2007).
2. Y. Wang, S. Zhang, and J. H. Oliver, Opt. Express **19**, 8539 (2011).
3. L. Lu, J. Xi, Y. Yu, and Q. Guo, Opt. Express **21**, 30610 (2013).
4. Z. Wang and B. Han, Opt. Lett. **29**, 1671 (2004).
5. X. F. Xu, L. Z. Cai, X. F. Meng, G. Y. Dong, and X. X. Shen, Opt. Lett. **31**, 1966 (2006).
6. C. Guo, B. Sha, Y. Xie, and X. Zhang, Opt. Lett. **39**, 813 (2014).
7. Z. Zhang, IEEE Trans. Pattern Anal. Mach. Intell. **22**, 1330 (2000).
8. S. Zhang and P. S. Huang, Opt. Eng. **45**, 083601 (2006).
9. R. Juarez-Salazar, C. Robledo-Sanchez, F. Guerrero-Sanchez, and A. Rangel-Huerta, Opt. Express **22**, 4738 (2014).